STUDIA UNIVERSITATIS BABEŞ-BOLYAI, CHEMIA, LIII, 2, 2008

BASIC TESSELLATIONS IN NANOSTRUCTURES

MIRCEA V. DIUDEA*

ABSTRACT. Basic tessellations in nanostructures, like the polyhex (6,3) and pattern, encountered in nanotubes and tori as well as the fullerene coverings derived from the Platonic solids can be performed by two main procedures, implemented in three original software programs developed at the TOPO Group Cluj: the cut procedure, suitable for tubular structures covering and the map operations, for spherical structures. Correspondence between Cluj-like and the classical notation of tubular structures is clearly demonstrated. Parameters of the transformed networks are given in terms of the primitive lattice vectors and original cage covering. Electronic structure of at the simple π-Hückel accounts for the metallic or insulating behavior of tubular structures. Covering criteria for metallic character in polyhex tori are derived from the network parameters. Formulas for the iterative operations on maps of vertex degree three are presented.

INTRODUCTION

Covering a surface by various polygonal or curved regions is an ancient human activity. It occurred in house building, particularly in floor, windows and ceiling decoration. There were well known three regular Platonic tessellations (*i.e*., coverings by a single type face and a single vertex degree): (4,4), (6,3) and (3,6). The Greek and Roman mosaics were very appreciated in this respect.

Covering is nowadays a mathematically founded science.[1-4] Covering modification is one of the ways in understanding chemical reactions occurring in nanostructures, particularly in carbon allotropes. Nanostructure modeling necessarily involves the embedding of a polygonal lattice in a given 3D surface *S*. Such a "combinatorial" surface is called a map *M*. Analytical formulas, for generating a smooth surface, can be found in Mathematical recipes, available on internet. The coordinates of the lattice points are obtained by partitioning *S*, either by dedicated algorithms or by simply drawing vertices and edges on display, with the aid of some builders to switch from 2D to 3D. Another way uses templates, *e.g*., unit blocks with a prescribed spatial arrangement. The TOPO Group Cluj has developed three main software programs TORUS [5] CageVersatile [3] (CVNET) and JSCHEM [6].

* *Faculty of Chemistry and Chemical Engineering, "Babeş-Bolyai" University, 400028, Cluj, Romania*

SQUARE (4,4) LATTICE

The embedding of the (4,4) net is made by circulating a *c*-fold cycle, circumscribed to the toroidal tube cross-section, along the cylinder or around the large hollow of the torus. The subsequent *n images* of *c*-fold cycle, equally spaced are joined with edges, point by point, to form a polyhedral cylinder/ torus tiled by a tetragonal pattern. Twisted, chiral, (4,4) tori can be generated by the following two procedures: [4,7] (1) twisting the horizontal layer connections (Figure 1a) and (2) twisting the vertical layer (offset) connections (Figure 1b).

(a) T(4,4)H2[8,24] (b) T(4,4)V2[8,24]

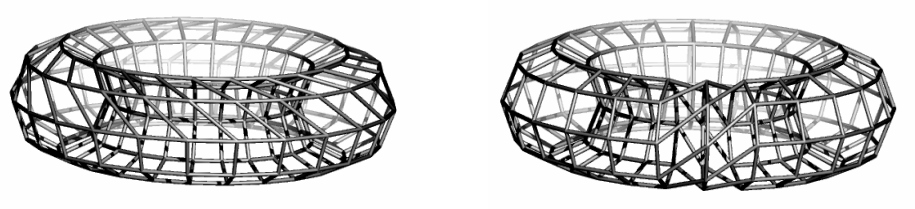

Figure 1. An H-twisted (a) and a V-twisted (b) embedding of the (4,4) net.

POLYHEX (6,3) NETWORK

To obtain the (6,3) tessellation,[1,4,7] each second edge of the (4,4) net has to be cut off. Two isomeric embeddings can be defined in the torus. Two topologically distinct tori are obtained by the TORUS program: T(6,3)H/Z[*c*,*n*] and T(6,3)V/A[*c*,*n*] and they correspond to two different classes of aromatic chemical compounds, phenacenes and acenes, respectively. The H-embedding is obtained when the cut edges lye horizontally (*i.e*., perpendicular to the Z axis of the torus). It is also called “zigzag” Z, by the tube cross-section shape. The V-embedding results when the cut edges lye vertically (*i.e*., parallel to the Z axis of the torus). It is also called “armchair” A, by the tube cross-section aspect. The name of such tori is a string of characters including the tiling, type of embedding and the tube dimensions [*c*,*n*].

By performing a cross-section on a polyhex torus (or by using the cylinder to embed a (4,4) net leading ultimately to the (6,3) pattern) and next optimizing, by a Molecular Mechanics procedure, the generated polyhex tubes and tori look like in Figure 2. The objects in these examples represent non-chiral structures.

Each of the twisting of the (4,4) tori (Figure 1) lead to four classes [7] of twisted tori: (i) H-twist, H-cut HH*t*[*c*,*n*]; (ii) H-twist, V-cut, HV*t*[*c*,*n*]; (iii) V-twist, H-cut, VH*t*[*c*,*n*]; and (iv) V-twist, V-cut, VV*t*[*c*,*n*]. The type of cutting will dictate

the type of embedding and, ultimately, the shape of objects. Conversely, the type of twisting is involved in the π-electron structure of polyhex tori. Figure 3. illustrates some (non-optimized) twisted polyhex tori.

(a) Tu(6,3)V/A[12,12]; v = 144 (b) T(6,3)H/Z[12,50]; v = 600

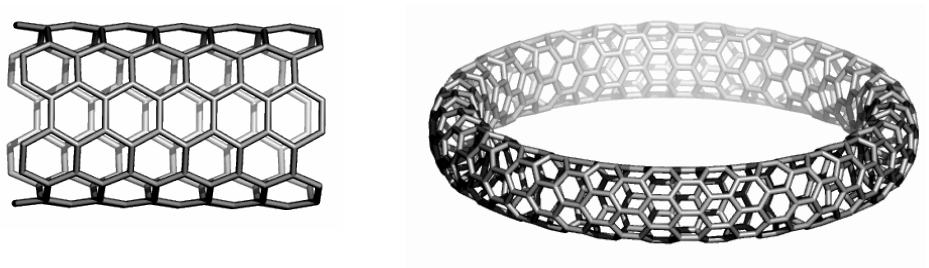

Figure 2. The (6,3) covering in the cylindrical (a) and toroidal (b) embedding, respectively.

The twist number t is just the deviation (in number of hexagons) of the chiral (*i.e*., rolling-up) vector to the zigzag line, in the graphite sheet representation [8-11] Accordingly, a torus can be drawn as an equivalent planar parallelogram, involving two tubes: one tube is built on the rolling-up vector R (Figure 3.7), which, in terms of the primitive graphite lattice vectors, is written as:

T(6,3)HH2[8,24] T(6,3)VH2[8,24] (offset)

T(6,3)HV2[8,24] T(6,3)VV2[8,24] (offset)

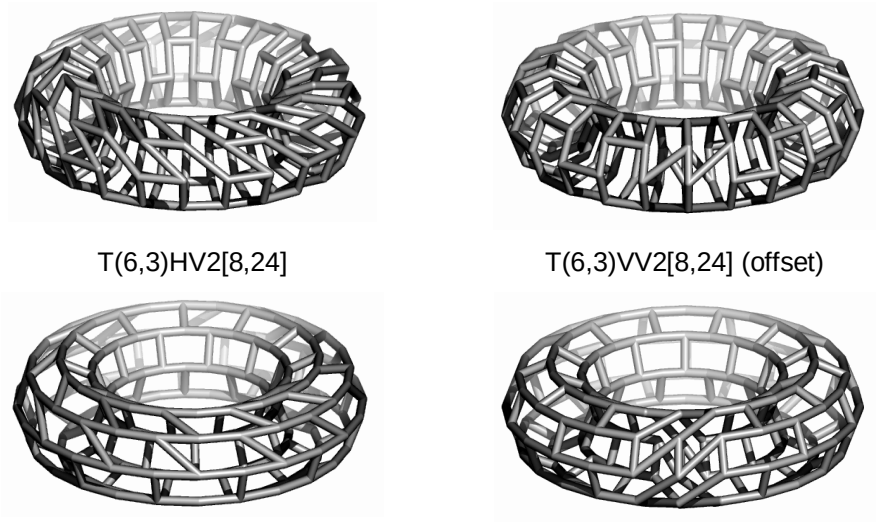

Figure 3. The four classes of twisted polyhex tori (non-optimized).

$$R = ka_1 + la_2 \quad (1)$$

The second tube is formally defined on the translating vector *T*:

$$T = pa_1 + qa_2 \quad (2)$$

For a given torus, the first tube can be identified by cutting the object across the tube while the second one results by cutting it around the large hollow. Anyway, a four integer parameter description (*k*,*l*,*p*,*q*) can be written. The coordinates of THH4[14,6] torus depicted in Figure 4 are: [7] (5, -4, 3, 3). Note that this representation is not unique and is reducible to three parameter notation, theorized by Kirby *et al* [9,12].

Correspondence between our notation for tubes (TUX*t*[*c*,*n*]) and tori (TX*t*[*c*,*n*]) and that in two (*k*,*l*) and four (*k*,*l*,*p*,*q*) integers notation are given in Tables 1 and 2, respectively.

Table 1.

Correspondence between the TUX*t*[*c*,*n*] and (*k*,*l*) notation.

	Tube X*t*	(*c*,*t*); (*k*,*l*)	Tube (*k*,*l*)
1	H	*c*=2*k*; *t*=*l*=0	(*c*/2,0); Z
2	HH*t*	*c*=*k*+2*l*; *t*=*k*; *l*=(*c*-*t*)/2	[*t*,(*c*-*t*)/2]
3	HV*t*	*c*=*k*+*l*; *t*=*k*; *l*=*c*-*t*	[*t*,(*c*-*t*)]
4	V	*c*=2*k*; *t*=*l*=0	(*c*/2,*c*/2); A

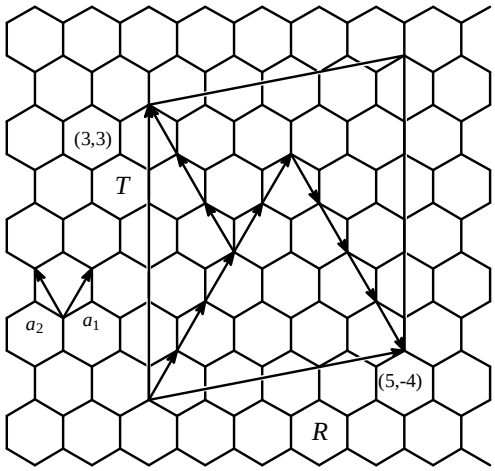

Figure 4. Representation of the torus THH4[14,6] by an equivalent parallelogram defining two tubes: one defined on the rolling-up vector *R* (with integer coordinates (*k*,*l*)) and the other on the translating vector *T* (given by the pair (*p*,*q*)). The four parameter specification of the depicted torus is (5, -4, 3, 3).

Table 2.

Correspondence between the TX*t*[*c*,*n*] and (*k*,*l*,*p*,*q*) notation.

	Torus X*t*	Tube *R*	Tube *T*	Torus (*k*,*l*,*p*,*q*)*	*v*
1	H	H/Z	V/A	$(c/2,-c/2,n/2,n/2)$	$2(kq-lp)=cn$
2	V	V/A	H/Z	$(c/2,c/2,n/2,-n/2)$	$2(lp-kq)=cn$
3	HH*t*	HH (tw)	V/A	$[(c-t)/2,-t,n/2,n/2]$	$2(2kq-lp)=cn$
4	HV*t*	HV (tw)	H/Z	$[(c+t)/2,(c-t)/2,n/2,-n/2]$	$2(lp-kq)=cn$
5	VH*t* (offset)	H/Z	HV (tw)	$[c/2,-c/2,(n+t)/2,(n-t)/2]$	$2(kq-lp)=cn$
6	VV*t* (offset)	V/A	HH (tw)	$[c/2,c/2,(n-t)/2,-t)]$	$2(2lp-kq)=cn$

* First pair (*k*,*l*) denotes the rolling-up vector *R* while last pair (*p*,*q*) specifies the translating vector *T*. The representation (*m*,-*m*) = (*m*,0), is an H/Z-tube while (*m*,*m*) is a V/A-tube.

π-ELECTRONIC STRUCTURE OF POLYHEX TORI

In the Spectral Theory, at the simple π-only Hückel [13] level of theory, the energy of the i^{th} molecular orbital $E_i = \alpha + x_i\beta$ is evaluated by calculating the solutions x_i of the characteristic polynomial *Ch*(*G*,*x*) or the eigenvalues of the adjacency matrix associated to the molecular hydrogen depleted graph.

The π-electronic shells of neutral graphitic objects are classified [14,15] function of their eigenvalue spectra, as *closed*, when $x_{v/2} > 0 \geq x_{v/2+1}$ or *open*, when the HOMO and LUMO molecular orbitals are degenerate, $x_{v/2} = x_{v/2+1}$.

The *metallic* character involves the existence of a zero HOMO-LUMO gap (a particular case of the open shell) and the degeneracy of some non-bonding orbitals [16] (NBOs) favoring the spin multiplicity, cf. the Hund rule. In polyhex tori, the metallic behavior is ensured by *four* NBOs, also present in the graphite sheet. The gap (in β units) is taken as the absolute value of the difference E_{HOMO} - E_{LUMO}. Table 3 gives the lattice [*c*,*n*] criteria (in terms of our notation) for metallic shell in (6,3) tori of various types.

Table 3.

Covering criteria for metallic character in polyhex tori

	Torus	Metallic
	Non-Twisted	
1	H/Z[*c*,*n*]	0 mod (*c*,6)
2	V/A[*c*,*n*]	0 mod (*n*,6)
	H-Twisted	

3	HH*t*[*c*,*n*]	0 mod (*c*,6)
4	HV*t*[*c*,*n*]	0 mod (*n*,6) 0 mod(*t*,6)
	V-Twisted	
5	VH*t*[*c*,*n*]	0 mod (*c*,6) 0 mod (*t*,6)
6	VV*t*[*c*,*n*]	0 mod (*n*,6)

OPERATIONS ON MAPS

Modifying a covering is one of the ways in understanding chemical reactions occurring in nanostructures, particularly in carbon allotropes [17-20].

A map *M* is a combinatorial representation of a (closed) surface [21]. Let us denote in a map: *v* – the number of vertices, *e* - the number of edges, *f* – the number of faces and *d* – the vertex degree. A subscript "0" will mark the corresponding parameters in the parent map. The famous EULER (1758) formula: [22,23]

$$v - e + f = \chi(M) = 2(1-g) \tag{3}$$

with χ being the Euler *characteristic* and *g* the genus [24] of a graph is useful for checking the consistency of an assumed structure. Positive/negative χ values indicate positive/negative curvature of a lattice.

Some geometrical-topological transformations, called operations on maps, are used to relate parents and transformed associate graphs of nanostructures. In this respect, operations such as: dualization *Du*, medial *Me*, truncation *Tr*, polygonal P_r capping or Snub Sn, are well known. Among the five Platonic solids, Tetrahedron is self-dual, and the remainders form dual pairs: Cube-Octahedron and Dodecahedron-Icosahedron (Figure 5).

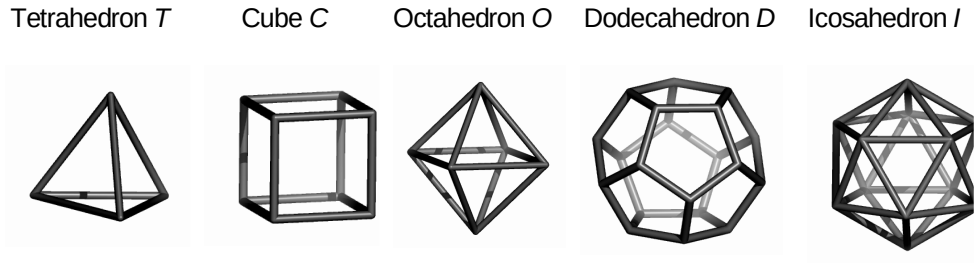

Figure 5. The five Platonic polyhedra.

Some other operations can be derived ac combinations of the simplest ones. In the following, three of the most important composite operations on maps are presented.

Leapfrog *Le*. Leapfrog (*tripling*) is a composite operation [25-32] that can be written as:

$$Le(M) = Du(P_3(M)) = Tr(Du(M)) \quad (4)$$

A sequence of stellation-dualization rotates the parent *s*-gonal faces by π/s. Leapfrog operation is illustrated, on a pentagonal face, in Figure 6.

A bounding polygon, of size $2d_0$, is formed around each original vertex. In the most frequent cases of 4- and 3-valent maps, the bounding polygon is an octagon and a hexagon, respectively.

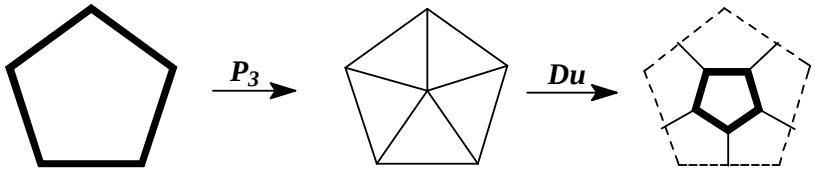

Figure 6. The Leapfrog *Le* operation on a pentagonal face

The number of vertices in Le(M) is d_0 times larger than in the original d_0 regular map M, irrespective of the tessellation type. The complete transformed map parameters are:

$$Le(M): \quad v = s_0 f_0 = d_0 v_0; \quad e = 3e_0; \quad f = v_0 + f_0 \quad (5)$$

Note that in *Le*(*M*) the vertex degree is *always* 3, as a consequence of the involved triangulation P_3. In other words, the dual of a triangulation is a *cubic net* [21]. A nice example of using *Le* operation is: *Le*(Dodecahedron) = Fullerene C_{60} (Figure 7). The leapfrog operation can be used to insulate the parent faces by surrounding bounding polygons.

Dodecahedron *D*; *v* = 20 Fullerene C_{60} ; *v* = 60

Figure 7. Realization of *Le* operation

Chamfering *Q*. Chamfering (quadrupling) [30-33] is another composite operation, written as the sequence:

$$Q(M) = RE(Tr_{P_3}(P_3(M))) \tag{6}$$

where *RE* denotes the (old) edge deletion (dashed lines, in Figure 8) in the truncation Tr_{P3} of each central vertex of the P_3 mapping. The *Q* operation leaves unchanged the initial orientation of the polygonal faces.

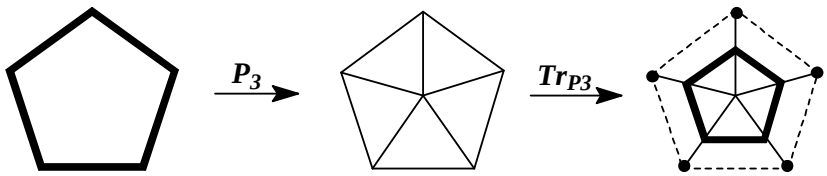

Figure 8. The Quadrupling *Q* operation on a pentagonal face.

The vertex multiplication ratio in a Q transform is d_0+1 irrespective of the parent map tessellation. The complete transformed parameters are:

$$Q(M):\ v = (d_0 + 1)v_0;\ \ e = 4e_0;\ \ f = f_0 + e_0 \tag{7}$$

Q operation involves two π/s rotations, so that the initial orientation of the polygonal faces is preserved. Note that, because of preserving the old vertices, *Q*(*M*) is, in general, non-regular; only in case of a 3-valent *M*, *Q*(*M*) is a 3-regular graph and vertex multiplication is 4 (from which the name *quadrupling* is derived. *Q* insulates the parent faces always by hexagons. An example of this operation is: *Q* (Dodecahedron) = Fullerene C_{80} (Figure 9).

Dodecahedron *D*; *v* = 20

Fullerene C_{80} ; *v* = 80

Figure 9. Realization of *Q* operation

Capra *Ca.* Capra operation is a composite operation that can be written as a sequence of simple operations: [1,4,7,34-38]

$$Ca(M) = Tr_{P_5}(P_5(M)) \tag{8}$$

with Tr_{P5} meaning the truncation of new, face centered, vertices introduced by P_5 pentagonal mapping (Figure 10).

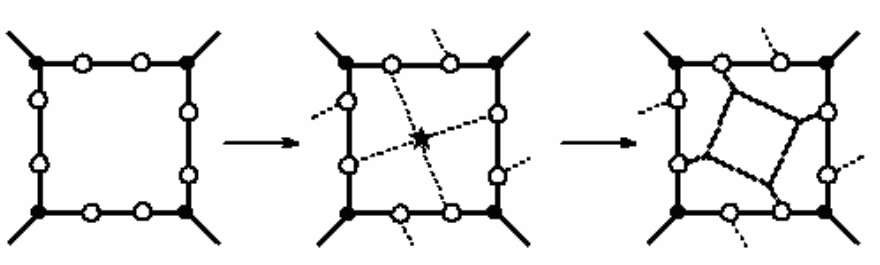

Figure 10. The Capra operation on asquare face.

The nuclearity of the Goldberg (1937) polyhedra [33] (related to the fullerenes) is given by the parameter:

$$m = (a^2 + ab + b^2);\ a \geq b;\ a + b > 0 \tag{9}$$

which is the multiplication factor $m = v/v_0$: in a 3-valent map, *Le* ((1,1); $m = 3$; *Q* ((2,0); $m = 4$ and *Ca*((2,1); $m = 7$. The m factor was used since the ancient Egypt for calculating the volume of truncated pyramid, of height h: $V = mh/3$.

Ca insulates any face of *M* by its own hexagons, which are not shared with any old face. It is an intrinsic chiral operation [37] (it rotates the parent edges by $\pi/(3/2)s$. Since pentangulation of a face can be done either clockwise or counter-clockwise, it results in an enantiomeric pair of objects: $Ca_S(M)$ and $Ca_R(M)$, with the subscript *S* and *R* given in terms of the *sinister*/*rectus* stereochemical isomerism.

The vertex multiplication ratio in the *Ca* operation is $2d_0 + 1$ irrespective of the original map tiling. The transformed map parameters are shown in the following relations:

$$Ca(M):\ v = v_0(2d_0 + 1);\ e = 7e_0;\ f = f_0(s_0 + 1) = 2e_0 + f_0 \tag{10}$$

The iterative n-time operating (on maps with vertex degree $d_0 = 3$) leads to the following transformed lattice parameters: [4,7]

$$v_n = 7^n v_0;\ \ e_n = 7^n e_0;\ \ f_n = f_0(s_0(7^n - 1)/6 + 1) \tag{11}$$

An example of molecular realization of *Ca* operation (applied on the Dodecahedron) is the chiral fullerene C_{140} (Figure 11).

C_{140}

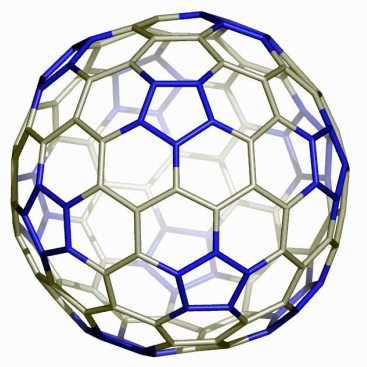

Figure 11. Realization of the Capra *Ca* operation

REFERENCES

1. M. V. Diudea, Covering forms in nanostructures, *Forma* (Tokyo), **2004**, *19*, 131.
2. M. V. Diudea and P. E. John, A. Graovac, M. Primorac, and T. Pisanski, *Croat*. *Chem*. *Acta*, **2003**, *76*, 153.
3. M. Stefu and M. V. Diudea, *CageVersatile* 1.3, "Babes-Bolyai" University, 2003.
4. M. V. Diudea and Cs. L. Nagy Cs. L., *Periodic nanostructures*, Springer, Chap. 6, 2007.
5. M. V. Diudea, B. Parv and O. Ursu, TORUS, "Babes-Bolyai" University, 2001.
6. Cs. L. Nagy, M. V. Diudea, JSCHEM, "Babes-Bolyai" University, 2004.
7. M. V. Diudea, Ed., *Nanostructures, novel architecture*, NOVA, N. Y., 2005.
8. A. Ceulemans, L. F. Chibotaru, and P. W. Fowler, *Phys*. *Rev*. *Lett*., **1998**, *80*, 1861.
9. E. C. Kirby, R. B. Mallion, and P. Pollak, *J*. *Chem*. *Soc*. *Faraday Trans*., **1993**, *89*, 1945.
10. S. A. Bovin, L. F. Chibotaru, and A. Ceulemans, *J*. *Molec*. *Catalys*., **2001**, *166*, 47.
11. N. Hamada, S. Sawada, and A. Oshiyama, *Phys*. *Rev*. *Lett*., **1992**, *68*, 1579.
12. E. C. Kirby and P. Pollak, *J*. *Chem*. *Inf*. *Comput*. *Sci*., **1998**, *38*, 66.
13. E. Hückel, *Z*. *Phys*., **1931**, *70*, 204.
14. P. W. Fowler, *J*. *Chem*. *Soc*., *Faraday Trans*., **1997**, *93*, 1.
15. P. W. Fowler, *J*. *Chem*. *Soc*., *Faraday Trans*., **1990**, *86*, 2073.
16. M. Yoshida, M. Fujita, P. W. Fowler, and E. C. Kirby, *J*. *Chem*. *Soc*., *Faraday Trans*., **1997**, *93*, 1037.

17. D. J. Klein and H. Zhu, in: *From Chemical Topology to Three - Dimensional Geometry* (Ed. A. T. Balaban), Plenum Press, New York, 1997, pp. 297.
18. M. Deza, P. W. Fowler, M. Shtorgin, and K. Vietze, *J. Chem. Inf. Comput. Sci.*, **2000**, *40*, 1325.
19. B. de La VaissiÈre, P. W. Fowler, and M. Deza, *J. Chem. Inf. Comput. Sci.*, **2001**, *41*, 376.
20. P. W. Fowler and T. Pisanski, *J. Chem. Soc. Faraday Trans*., **1994**, *90*, 2865.
21. T. Pisanski and M. Randić, in *Geometry at Work*, (Ed. C. A. Gorini) M. A. A. Notes, **2000**, ***53***, 174.
22. L. Euler, *Comment*. *Acad*. *Sci*. *I*. *Petropolitanae*, **1736**, *8*, 128.
23. L. Euler, *Novi Comment*. *Acad*. *Sci*. *I*. *Petropolitanae*, **1758**, *4*, 109.
24. F. Harary, *Graph Theory*, Addison-Wesley, Reading, MA, 1969.
25. V. Eberhard, *Zur Morphologie der Polyeder*, Leipzig,Teubner,1891.
26. P. W. Fowler, *Chem. Phys. Lett*., **1986**, *131*, 444.
27. P. W. Fowler and J. I. Steer, *J. Chem. Soc*., *Chem. Commun*., **1987**, 1403.
28. P. W. Fowler and K. M. Rogers, *J. Chem. Soc*., *Faraday Trans*., **1998**, *94***,** 1019.
29. P. W. Fowler, P. W. and K.M. Rogers, *J. Chem. Soc*., *Faraday Trans*., **1998**, *94***,** 2509.
30. M. V. Diudea and P. E. John, *MATCH*, *Commun. Math. Comput. Chem*., **2001**, *44*, 103.
31. M. V. Diudea, P. E. John, A. Graovac, M. Primorac, and T. Pisanski, *Croat. Chem. Acta*, 2003, *76*, 153.
32. A. E. Vizitiu, M. V. Diudea, S. Nikolić and D. Janežić, *J. Chem. Inf. Model.,* **2006**, *46*, 2574.
33. M. Goldberg, *Tôhoku Math. J*., **1937**, *43*, 104.
34. M. V. Diudea, *Studia Univ."Babes-Bolyai"*, **2003**, *48* (2), 3.
35. M. V. Diudea, *J. Chem. Inf. Model.,* **2005**, *45,* 1002.
36. R. B. King and M. V. Diudea, *J. Math. Chem*., **2005**, 38 (4), 425.
37. R. B. King and M. V. Diudea, *J. Math. Chem.* **2006**, *39*, 597.
38. M. V. Diudea, in: M. V. Diudea, Ed., *Nanostructures-Novel Architecture*, NOVA, New York, **2005**, 203.